Hole Transfer from Single Quantum Dots

Nianhui Song, Haiming Zhu, Shengye Jin, and Tianquan Lian*

Department of Chemistry, Emory University, Atlanta, Georgia 30322, United States

ABSTRACT Photoinduced hole transfer dynamics from single CdSe/CdS_{3ML}/$CdZnS_{2ML}$/ZnS_{2ML} core/multishell quantum dots (QDs) to phenothiazine (PTZ) molecules were studied by single QD fluorescence spectroscopy to investigate the static and dynamic heterogeneities of the hole transfer process as well as its effect on the blinking dynamics of QDs. Ensemble-averaged transient absorption and fluorescence decay measurements show that excitons in QDs dissociate by transferring the valence band hole to PTZ with a time constant of 50 ns for the 1:1 PTZ–QD complex, and the subsequent charge recombination process (*i.e.*, electron transfer from the conduction band of the reduced QD to oxidized PTZ to regenerate the complex in the ground state) occurs mainly on the 100 to 1000 ns time scale. Single QD–PTZ complexes show pronounced correlated fluctuations of fluorescence intensity and lifetime with time. In addition to the dynamic fluctuation, there are considerable heterogeneities of average hole transfer rate among different QD–PTZ complexes. The hole transfer process has little effect on the statistics of the off-states, which is often believed to be positively charged QDs with a valence band hole. Instead, it increases the probability of weakly emissive or "gray" states.

KEYWORDS: quantum dots · hole transfer · blinking dynamics · single particle spectroscopy

Understanding the dynamics of charge transfer from and to quantum dots (QDs) is essential to their potential application in solar cells.[1–4] For example, in QD solar cells based on QD-sensitized TiO_2 nanocrystalline thin films, the device performance depends on the efficiencies of the initial electron transfer from the QDs to TiO_2 and subsequent filling of the holes in the QD by the redox mediators, in addition to many other processes.[5] For this reason, exciton dissociation in CdX and PbX (X = S, Se, and Te) QDs by ultrafast electron transfer (ET) to molecular electron acceptors or semiconductors has been investigated.[5–19] Examples of hole transfer (HT) are relatively few, and the rate of hole transfer is considerably slower for reasons yet to be understood.[20–24] Much of our understanding of ET dynamics from QDs is derived from ensemble-averaged measurements, which show that these processes are highly heterogeneous. Further insights into the heterogeneity of ET dynamics have been gained through studies of electron transfer of single QD–electron acceptor complexes.[25–31] Interestingly, the ET activity in these complexes is intermittent, modulated by the blinking dynamics of single QDs.[25–31] Because of the important roles of these interfacial electron and hole transfer activities in QD–solar cells, further studies of their dependences on single QD blinking dynamics are needed.

Under continuous excitation, single QDs fluctuate between on-states (with high fluorescence intensity and long lifetime) and off-states (with low fluorescence intensity at or near the background level and short lifetimes).[25,27,28,32–54] The off-states have been attributed to photoinduced charging of QDs by Auger ionization and/or electron transfer to trap states in QDs or the surrounding matrix.[32–34,36,45,48,53,54] The probability densities of the on- and off-times obey a power-law distribution with an exponent of ~1.5,[33,36,55,56] and this dependence can be explained by models that assume diffusion-controlled electron transfer (ET).[33,48,52,53,56–58] These models suggest that the blinking dynamics can be suppressed by a number of approaches, including filling of the electron trap states (by surface ligands[39,41,42] or n-doped semiconductors[28]), increasing the emission yield of the charged QD (by either increasing the radiative decay rate[36,44] or reducing the Auger recombination rate[38,40,59]) and decreasing the probability of accessing the off-states.[60,61] Despite these abilities to manipulate the blinking behavior, the nature of the trap states remains unclear and has yet to be systematically controlled.

Studying single QD–electron (or hole) acceptor complexes can provide important insight into the single QD blinking dynamics. In QD–electron (hole) acceptor complexes, the exciton dissociates by electron (hole) transfer to the acceptor, generating charge-separated states with the hole (electron) left in the QD. The effect of these charge-separated states on the blinking dynamics can be used to probe the nature of the off-states. Furthermore, in QD–acceptor complexes,

* Address correspondence to tlian@emory.edu.

Received for review July 18, 2011 and accepted October 2, 2011.

Published online October 03, 2011
10.1021/nn202713x

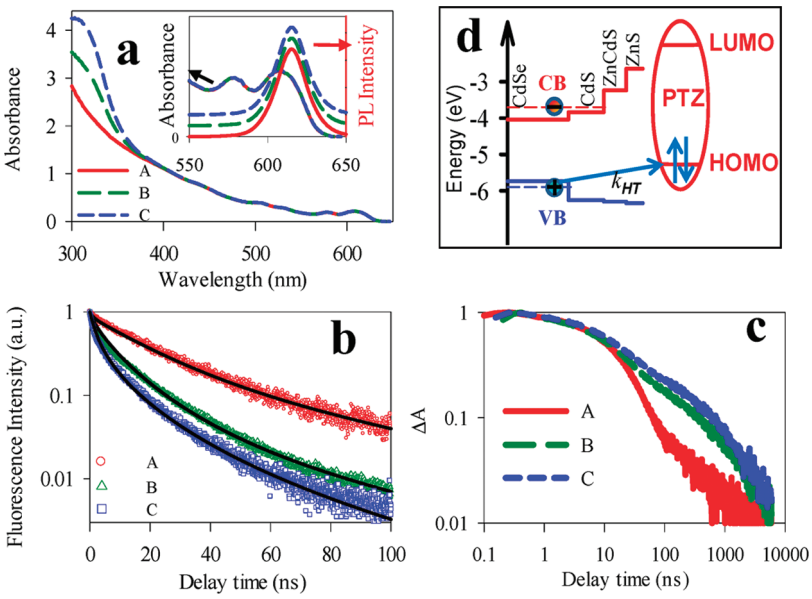

Figure 1. (a) UV−vis absorption spectra (dashed lines), (b) ensemble-averaged fluorescence decays (open symbols), and (c) 1S exciton bleach recovery kinetics of QD−PTZ complexes of samples A (red, free QDs), B (green), and C (blue). The fluorescence spectra of the three samples are compared in the inset of panel a, along with an expanded view of the absorption spectra near the 1S exciton band. Solid lines in panel b are best fits according to the Poisson distribution model described in the text (eqs 1 and 2). (d) Energetic diagram of the QD−PTZ complex and possible charge transfer processes: hole transfer from the QD valence band (VB) to PTZ HOMO followed by charge recombination (not shown), in which the electron is transferred from the conduction band (CB) of the reduced QD to the oxidized PTZ.

the charge transfer rate can be controlled by the number as well as the nature of the acceptors, offering the possibility to test the relationship between the blinking dynamics and charge transfer rate. In recent studies of single QD−electron acceptor complexes, we and others have shown that the electron transfer rate and the blinking dynamics are correlated—the QDs exhibit larger probability of off-states in complexes with higher ET rate.[25−31] This finding supports the current model for the off-states because electron transfer to acceptors left a hole in the QDs, which is similar to the proposed off-state generated by Auger ionization or electron transfer to trap states. It also suggests that in QD−hole acceptor complexes, the presence of a hole transfer pathway may shorten the lifetime of off-states and therefore suppress the blinking dynamics. However, direct observations of the hole transfer process and correlations of the blinking dynamics with hole transfer rate on the single QD level have not been reported.

In this paper, we report a study of hole transfer dynamics in single QD−hole acceptor complexes. Ensemble-averaged transient absorption (TA) and fluorescence decay measurements confirm that in the QD−phenothiazine (PTZ, see Figure 2) complexes, excitons dissociate by hole transfer to PTZ, consistent with a previous study of related complexes.[20] At the single QD−PTZ level, QDs show correlated fluctuations of lifetime and intensity. The on-state fluorescence lifetime deceases, consistent with hole transfer. Unlike in an electron transfer process, the hole transfer pathway does not suppress the blinking or significantly alter the statistics of the on- and off-state distributions of QDs. Instead, it increases the probability of gray states. We propose a model to account for the observed effects of hole transfer on single QD blinking dynamics.

RESULTS AND DISCUSSION

Ensemble-Averaged Fluorescence Decays and Transient Absorption. We first examined the hole transfer and subsequent charge recombination processes by ensemble-averaged fluorescence decay and transient absorption measurements. CdSe/CdS_{3ML}/$CdZnS_{2ML}$/ZnS_{2ML} core/multishell QDs with a first exciton (1S) peak at 605 nm were used for this study. The ultraviolet−visible (UV−vis) absorption spectra of samples A, B, and C are displayed in Figure 1a. These spectra show the same QD absorption (from 400 to 605 nm) and different PTZ absorption (~320 nm), indicating a constant QD concentration and increasing PTZ-to-QD ratios from samples A (free QD without PTZ) to C. The exact ratios of adsorbed PTZ-to-QD could not be determined from the absorption spectra because the extinction coefficient of the QD is unknown and there is a partition of free and QD-bound PTZ molecules. As will be described below, these ratios can be estimated from the fluorescence decay kinetics of these samples. Both the exciton absorption and emission peak positions (see inset of Figure 1a) show negligible changes with increased PTZ-to-QD ratios.

Ensemble-averaged fluorescence decays of these samples are plotted in Figure 1b. These samples were

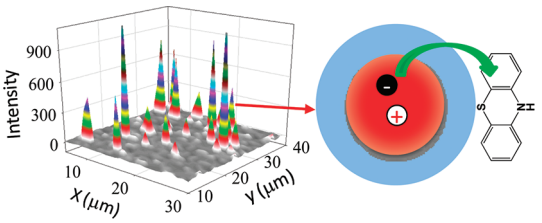

Figure 2. Raster scan fluorescence image of single QD−PTZ complexes on a glass coverslip and a schematic of the QD−PTZ complex.

excited at 500 nm, and the resulting QD emission from 540 to 625 nm was collected by time-correlated single photon counting. It is clear that exciton fluorescence decay is faster in QD−PTZ complexes than free QDs and the exciton quenching rate increases with the PTZ-to-QD ratio. Possible pathways for the observed exciton quenching in QD−PTZ complexes can be determined from the relative energy levels of QD and PTZ shown in Figure 1d. From the first exciton peak position of the QDs, the 1S electron and 1S hole levels can be estimated to be −3.89 and −5.79 V (relative to vacuum) according to the method reported in previous works.[28,62,63] The lowest unoccupied and highest occupied molecular orbital (LUMO and HOMO) levels of PTZ molecules were reported to be −1.6 and −5.5 V, respectively.[64] Exciton dissociation by ET from the QD to the PTZ LUMO level is energetically forbidden in this system. Energy transfer is not possible either due to the lack of spectral overlap of the QD emission with PTZ absorption. Hole transfer from the QD valence band to the HOMO of PTZ is energetically allowed and has been reported in our previous work.[20]

Exciton quenching by hole transfer generates a charge-separated state with a reduced QD and oxidized PTZ radical. The 1S electron in the reduced QD can eventually recombine with the hole at the HOMO level of the oxidized PTZ radical to regenerate the complex in the ground state. To probe this charge recombination process and to provide further evidence for the HT pathway, we have also carried out transient absorption study of the QD−PTZ complexes. As shown in Figure 1c and Figure S1 (Supporting Information), in samples A, B, and C, excitation by 400 nm pulses generates excited QDs, in which the filling of the 1S electron level leads to the bleach (or decrease of absorption) of the 1S exciton band.[20,65,66] The 1S exciton bleach recovery kinetics directly monitors the removal rate of the 1S electron. In QD−PTZ complexes, the QD 1S exciton bleach shows a slower recovery (or longer lived 1S electron on the 10 ns to a few microseconds scale) than the free QDs. It indicates that in the QD−PTZ complexes, excitons dissociate by HT from the QD to PTZ, which increases the lifetime of the 1S electron by removing the 1S electron−1S hole recombination pathway. Exciton quenching by both electron and energy transfers would have shortened the 1S electron lifetime. Furthermore, it was previously shown that in CdSe QD−PTZ complexes, the decay of the QD 1S exciton fluorescence leads to the formation of PTZ radicals (at ∼520 nm), directly confirming the interfacial HT process.[20] In the current system, the overlap of the strong exciton bleach signatures with the much weaker PTZ radical absorption hinders a direct measurement of the latter. The recovery of 1S exciton bleach in the QD−PTZ complex on the 100 ns to a few microseconds time scale is assigned to the charge recombination process, transferring the 1S electron to the PTZ radical to regenerate the complex in the ground state.

HT Dynamics in Single QD−PTZ Complexes. To examine the effect of hole transfer on the blinking dynamics of single QDs, we examine three samples (1−3) of QD−PTZ complexes by single QD fluorescence spectroscopy. The PTZ-to-QD ratios, controlled by the amount of PTZ added, increase from sample 1 (free QD) to sample 3. A raster scan fluorescence image of single QD−PTZ complexes is shown in Figure 2, indicating spatially well-separated single QD−PTZ complexes. About 40−50 single QDs from each sample were detected, and each QD was followed for about 5 min. Two times associated with each detected photon, the delay time (relative to excitation pulse) and the arrival time (relative to the start of the experiment), were recorded. For each QD, an intensity trace was constructed by counting the number of photons within 50 ms arrival time windows. The delay time histograms of photons within 1 s arrival time windows were constructed and fitted to single-exponential decay functions (by nonlinear least-squares fit) to obtain the lifetime trajectory. Typical intensity and lifetime trajectories of single QD and QD−PTZ complexes from these samples are shown in panels b1−b3 of Figure 3. Typical fluorescence decay curves at selected times along the trajectories shown in panels b2 and b3 of Figure 3 are shown in Figure S2 (Supporting Information). All trajectories show single-step bleaching of fluorescence intensity to the background level, consistent with the behavior of single emitters, although the possibility of a small number of aggregates of two or three emitters cannot be excluded. Recent studies show that aggregates of two or three nanorods show blinking statistics that are indistinguishable from single QDs, but different statistics are observed in aggregates with five or more nanorods.[67,68] The lifetime trajectory follows the intensity trajectory for both free QDs and QD−PTZ complexes, consistent with the reported positive correlation between the fluorescence intensity and lifetime of single QDs.[25,27,28,33,45−54] Intensity and lifetime histograms of these single QDs are plotted in Figure 3a,c, respectively. We attribute all points with intensity within six standard deviations of the background level to off-states and all points with higher intensities to on-states. The intensity threshold separating the "on" and "off"

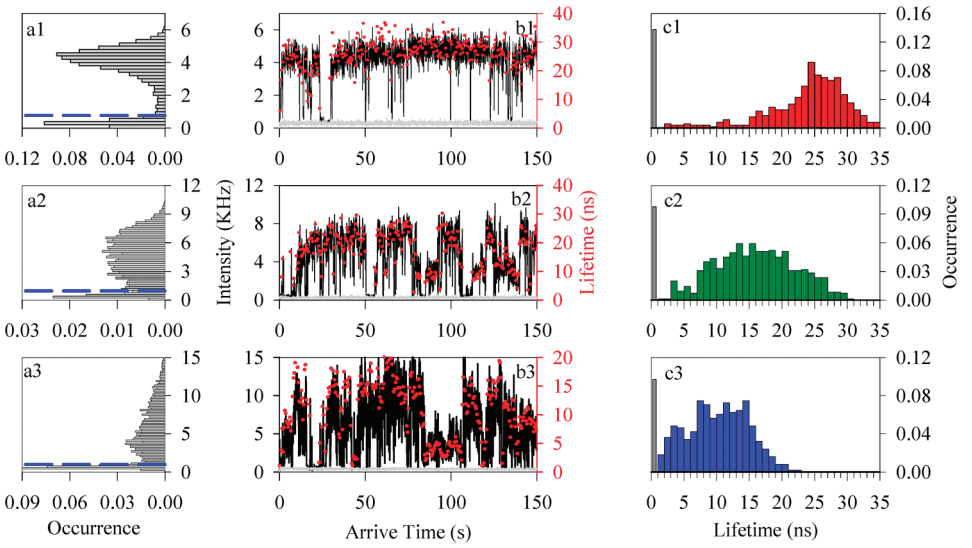

Figure 3. Typical fluorescence intensity (black line) and lifetime (red circles) trajectories (bi) and histograms of fluorescence intensity (with a 0.2 kHz bin) (ai) and lifetime (ci) of a representative single QD or QD−PTZ complex from each sample (i = 1−3 for samples 1−3, respectively). Blue dashed lines in (ai) indicate the threshold separating the on- and off-states. The gray lines in (bi) are the background emission level in this measurement. Black bars in (ci) indicate the occurrence of states with emission intensity at the background level, whose lifetime is estimated to be smaller than 0.5 ns.

states are indicated by blue dashed lines in Figure 3a. For states with emission intensity at the background level, the exciton lifetimes cannot be accurately obtained because of limited photon numbers and are estimated to be smaller than 0.5 ns. The occurrences of these states are counted and plotted within the lifetime histograms in Figure 3c.

The total lifetime histograms constructed from 40, 50, and 50 QDs from samples 1, 2, and 3, respectively, are shown in Figure 4a. With increasing PTZ-to-QD ratios, the distribution of the on-state lifetimes shifts to the shorter lifetime region. This behavior is similar to what was observed in single QD−molecular electron acceptor complexes, in which the increase in exciton decay rate (due to electron transfer process) caused a decrease of the average on-state lifetime.[29,31] Similarly, in QD−PTZ complexes, hole transfer from the valence band of QDs to the HOMO of PTZ molecules results in the reduction of exciton lifetime, as shown by the ensemble-averaged measurement. On the single QD−PTZ level, this leads the observed shift of the on-state lifetime distribution to the shorter lifetime. For each QD and QD−PTZ complexes, an average exciton decay rate, defined as the inverse of the average on-state lifetime of each particle along its trajectory, was computed, from which histograms of average decay rates were constructed for each sample. As can be seen in Figure S3, the free QDs show relatively small variation of average decay rates between different QDs. The variation becomes bigger in QD−PTZ complexes. Because of the relatively narrow distribution of average intrinsic decay rate (k_0) of free QDs, the average HT rates for each QD−PTZ complex can be calculated by subtracting k_0 from the total

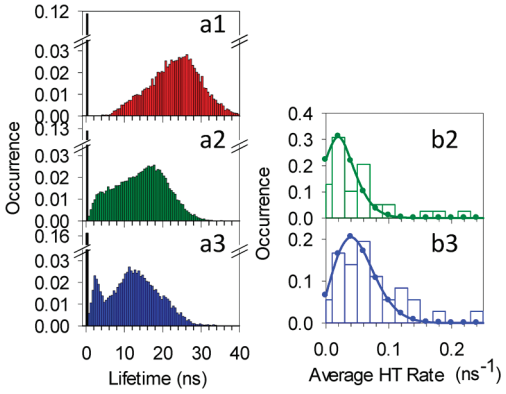

Figure 4. Histograms of total fluorescence lifetime distributions (ai) and average hole transfer rates (bi) for samples i (=1, 2, 3). Histograms of total lifetime distributions were constructed by summing up the lifetime distributions of all QDs in each sample. Black bars indicate the occurrence of low fluorescence intensity points along the trajectories, for which the lifetimes have been assumed to be 0.5 ns. The solid dots (connected by lines) in panels b2 and b3 are fits according to eq 1 with fitting parameters listed in Table 1.

decay rate k. As shown in Figure 4b, compared to sample 2, the distribution of average HT rates shifts to higher values in sample 3, consistent with the higher PTZ-to-QD ratio in this sample.

The distributions of the average HT rates are broad and asymmetric, showing a long tail in the high HT rate side. Similar asymmetric distributions of average ET rates were observed previously in QD−C60 complexes.[31] We have shown previously that in QD−molecular acceptor complexes prepared by self-assembly, the Poisson distribution of the number of adsorbates on the QD leads to Poisson distributions of average ET rates and fluctuations in single QD−adsobrate complexes and non-single-exponential ensemble-averaged fluoreseence decay

TABLE 1. Fitting Parameters for the Distributions of the Average HT Rates in Single PTZ–QD Complexes (Figure 4b) and the Ensemble-Averaged Fluorescence Decay of PTZ–QD Complexes (Figure 1c) According to Equations 1–3,[a]

single QD–C60 fluorescence decay				ensemble-averaged fluorescence decay	
k_1 (ns^{-1})	SD_1 (ns^{-1})	sample #	*m*	sample #	*m*
0.02	0.03	2	1.4	B	2.8
		3	2.5	C	3.4

[a] Values of k_1 and SD_1 are the average and standard deviation, respectively, of the HT rate in 1:1 PTZ–QD complexes; *m* is the average PTZ-to-QD ratio of the sample.

kinetics.[29,31] For the same reason, the number of adsorbed PTZs should also obey the Poisson distribution in the QD–PTZ complexes studied here.[20] Following this model, we assume that the number (*n*) of adsorbed PTZ molecule per QD obeys a Poisson distribution.[20,69,70] In *n*:1 PTZ–QD complexes, the average, k_n, and standard deviation, SD_n, of HT rates are given by $k_n = nk_1$ and $SD_n = nSD_1$, respectively, where k_1 and SD_1 denote the average and standard deviation of HT rates in the 1:1 PTZ–QD complexes. It can be shown that in a sample with an average PTZ-to-QD ratio of *m*, the distribution of the average HT rates of single PTZ–QD complexes is given by[29,31]

$$p(m; k_n) = \frac{m^{(k_n/k_1)} e^{-m}}{\left(\frac{k_n}{k_1}\right)!} \quad (1)$$

The total distribution of HT rates measured in an ensemble of single QD–PTZ complexes is

$$p(k_{HT}) = \sum_{n=1}^{\infty} \frac{m^n e^{-m}}{n!} \times \frac{1}{\sqrt{2\pi}(nSD_1)} e^{-(k_{HT} - nk_1)^2/2(nSD_1)^2} + e^{-m}\delta(k_{HT}) \quad (2)$$

Here the last term represents the contribution of free QDs (without adsorbates) in the PTZ–QD sample. In the ensemble-averaged fluorescence measurement, the distributions of HT rates from the individual PTZ–QD complexes are not explicitly measured and only the average fluorescence decay of all QDs is monitored. This ensemble-averaged fluorescence decay can be expressed as a sum of all single QD decays:[29,31]

$$[S(t)] = [S(0)][\int_0^{\infty} p(k_{HT}) e^{-k_{HT}t} dk_{HT}] f_{Free}(t) \quad (3)$$

Here $[S(t)]$ and $[S(0)]$ are the population of excited QDs at time *t* and 0, respectively; $f_{Free}(t)$ is the fluorescence decay of free QDs, which is independently measured and fitted.

The data shown in Figures 4b and 1c are fitted simultaneously by eqs 1 and 3, respectively. The same k_1 and SD_1 values are used for all samples, but the *m* values are allowed to change to reflect different average ratios in these samples. The histograms in Figure 4b were

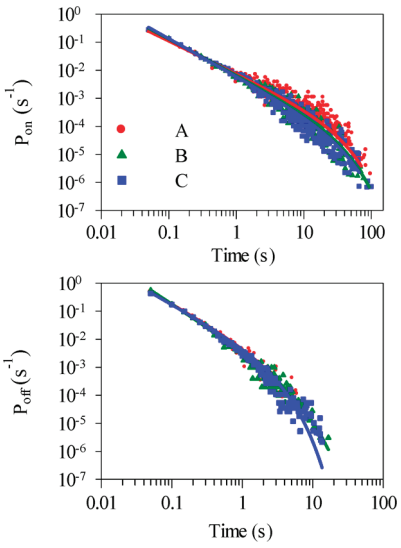

Figure 5. Probability density distributions of (a) on-states (P_{on}) and (b) off-states (P_{off}) as a function of on (off) time intervals, constructed from 40 free QDs from sample 1 (red circle), 50 complexes from sample 2 (green triangle), and 50 complexes from sample 3 (blue square). The solid lines are the best fits according to eq 5.

binned to reflect the value of k_1. This model leads to satisfactory fit to the data, as shown in Figures 4b and 1c, and the fitting parameters, *m*, k_1, and SD_1, are listed in Table 1. The HT rate in the 1:1 complexes is 2×10^{-7} s^{-1} (corresponding to a HT time of 50 ns). Our previous study showed that the hole transfer time in the 1:1 CdSe/PTZ complex is around 2.5 ns.[20] In the current system, the observed hole transfer rate is 20 times slower and it can be attributed to the retardation of HT rate by the multiple layers of insulating ZnS shells on the CdSe core.[71] From the average intrinsic decay rate of 5×10^{-7} s^{-1}, a hole transfer quantum yield of 29% in 1:1 PTZ–QD complexes can be estimated. This yield increases in complexes with more adsorbed PTZ molecules.

To examine the effect of the hole transfer process on the statistics of the single QD blinking dynamics, we have calculated the probability densities *P*(*t*) of a QD in the on- or off-states for a duration time of *t* according to eq 4.[33,48,52,53,56–58]

$$P_i(t) = \frac{N_i(t)}{N_{i,\,total}} \times \frac{1}{\Delta t_{avg}} (i = \text{on or off}) \quad (4)$$

Here, *N*(*t*) is the number of on- or off-events with duration time of *t*, N_{total} is the total number of on- or off-events, and Δt_{avg} is the average of the time intervals to the preceding and subsequent events. Recent studies have shown that the on- and off-time statistics can depend on the choice of threshold that separates the on- and off-states.[67,72–75] We have constructed on- and off-probability distributions using a thresholds of 0.6, 0.9, and 1.2 kHz, corresponding to the count rates at the background level plus 3, 6, and 9 standard deviations, respectively. As shown in Figure S4, within this range of threshold values, the on- and off-probability

TABLE 2. Fitting Parameters of $P_{on}(t)$ and $P_{off}(t)$ for All Single QDs from Samples 1, 2, and 3

sample #	α_{on}	$1/\Gamma_{on}$ (s)	α_{off}	$1/\Gamma_{off}$ (s)
1	1.17 ± 0.04	27 ± 3	1.5 ± 0.2	2.2 ± 0.1
2	1.28 ± 0.03	28 ± 3	1.6 ± 0.1	4.4 ± 0.3
3	1.34 ± 0.04	29 ± 3	1.2 ± 0.1	2.2 ± 0.1

distributions have negligible dependence on the choice of thresholds. We have chosen a threshold level of 0.9 kHz.

As shown in Figure 5, both $P_{on}(t)$ and $P_{off}(t)$ for single QDs from samples 1, 2, and 3 show power-law distributions at short time but deviate from this behavior at longer time, similar to results reported for free QDs and QD−electron acceptor complexes. These $P(t)$ distributions can be fit by a truncated power law:[33,48,52,53,56−58]

$$P_i(t) = B_i t^{-\alpha_i} \exp(-\Gamma_i t)\ (i = \text{on or off}) \qquad (5)$$

where B is the amplitude, α the power law exponent, and Γ the saturation rate. The fitting parameters are listed in Table 2. The probabilities of "on" time and "off" time in QD−PTZ complexes remain similar to bare QD and do not change significantly with PTZ-to-QD ratios. This indicates that the hole transfer process does not significantly affect the occurrence and the probability density distributions of the on- and off-states in QD−PTZ complexes within the limited time range (0.1 to 100 s for on-state and 0.1−10 s for off-state) probed in this experiment. This observation is different from QD−molecular electron acceptor complexes, where the possibilities of long on (off) and short off (on) events deceases (increases) with molecule-to-QD ratios (or electron transfer rates).[29,31]

A closer inspection of the total lifetime histograms in Figure 4a shows a significant increase in states with lifetime between 1 and 5 ns in QD−PTZ complexes compared to free QDs. These states, often labeled as "gray states",[38,40,59,76,77] fall between the high intensity region of the off-state distribution and the low intensity of the on-state distribution. The increase of gray states affects both the on- and off-states, which may account for the lack of changes in the probability distributions of on- and off-states in the presence of the HT pathway.

The experimental findings of the single QD−PTZ complex studies are the following: (1) The HT process shortens the average lifetime of the on-states. (2) The presence of the HT pathway does not significantly alter the occurrence of off-states. Instead, it increases the probability of "gray" states with lifetimes between 1 and 5 ns. To account for effect of the hole acceptor on the dynamics of single QDs, we propose a model for various states and their interconversion processes in the QD−PTZ complexes. As shown in Figure 6, when a neutral QD is excited from the ground state (**1**), an on-state (**1***) is generated, which can relax to state **1** by

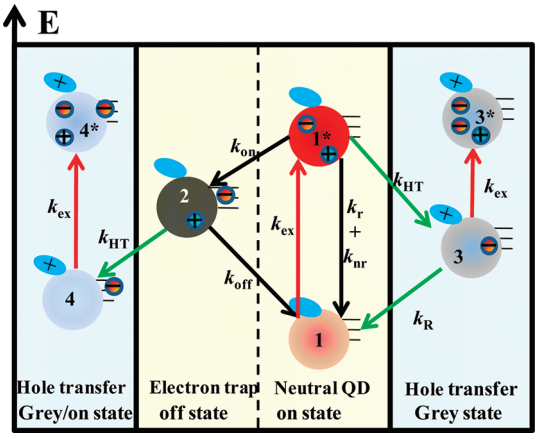

Figure 6. Possible states and charge transfer processes in QD−PTZ complexes. On-states 1 and 1* are the ground and excited states of the neutral QD−PTZ complex; k_{ex} is the excitation rate of QDs, and k_r and k_{nr} are intrinsic radiative and nonradiative decay rates of QDs. Electron ionization or transfer to trap state converts (with rate constant k_{on}) 1* to state 2 (off-state), which can convert back (with rate constant k_{off}) to the on-state by charge recombination. In the presence of hole acceptors, two additional pathways are created. 1* can be quenched by hole transfer to the hole acceptor (with rate constant k_{HT}), forming state 3. State 3 is a gray state because upon its excitation a negative trion is generated inside the QD, which has a low but detectable emission quantum yield. Hole transfer from the off-state (2) generates state 4, which should be emissive.

intrinsic radiative or nonradiative relaxation with a total decay rate of approximately 10^8−10^7 s^{-1}. As the QD cycles between the excitation and emission processes, there is a chance for the excited electron to be transferred to trap states in or near the QD (with rate constant k_{on}), thus forming the off-state (state **2**). The emission quantum yield for QDs in state **2** is at or near the background level because optical excitation of state **2** generates a positive trion which relaxes *via* a rapid nonradiative Auger recombination process (not shown).[66] When the trapped electron recombines with the positively charged QD (rate constant k_{off}), state **1** is regenerated. These states and rate constants for their interconversion are assumed to be the same in free QDs and QD−PTZ complexes.

The presence of hole acceptors creates two additional states and pathways for their interconversion. Hole transfer process from the excited neutral QD (state **1***) generates a charge separated state (state **3**) consisting of a PTZ cation and a negatively charged QD with a conduction band electron. Excitation of **3** generates a negative trion state in the QD, similar to the one studied by Jha and Sionnest.[78] These authors show that trions in CdSe/CdS QDs with core diameter around 4 nm have a total lifetime of 0.7−1.5 ns and a radiative decay rate of 10^8 s^{-1}, which should have weak but detectable emissions under single QD conditions. Therefore, we attribute this charge-separated state (**3**) to the gray state. This state can relax back to the ground state (**1**) by transferring the electron from the

QD to oxidized PTZ (*i.e.*, the charge recombination process), with a rate constant of $10^6 \sim 10^7$ s^{-1} as determined by the TA kinetics shown in Figure 1c. The TA data also show that the charge-separated state has a highly dispersive decay process, with a small but non-negligible probability for existing beyond 6 μs (the longest time measured in the transient study). Thus, it is possible that the increased probability of gray states observed in the experiment can be attributed to the charge-separated state (with negatively charged QDs) generated by the hole transfer process.

The presence of the hole acceptor is also expected to remove the hole in the dark sate (**2**), converting to state **4**, which is a neutral QD with adsorbed PTZ cation and a trapped electron on the QD surface. This state should be emissive upon excitation, and therefore, this process should alter the fate of the dark state and the distribution of the off-state probability density. However, as shown in Figure 5, the on- and off-state distributions have not been significantly changed in the current system. The reason for this is unclear. We tentatively attribute this to the competing effects of the hole acceptors on the off-state distribution of QDs. On one hand, it can remove the off-state (**2**) by transferring the hole to the acceptors, reducing the off-state probabilities. On the other hand, it can quench the excited QDs, generating the charge-separated state (**3**). As discussed above, this gray state has low emission quantum yield and can increase the probability of the off-states. Another possibility is that the hole in the dark state may also be trapped and cannot be effectively removed by PTZ because of reduced electronic coupling strength and driving force.[79] A trapped hole should have a reduced wave function overlap with the PTZ, decreasing the electronic coupling strength for HT. As shown in Figure 1d, the driving force for transferring the 1S hole to the PTZ is estimated to be ~0.3 eV. Trapping the hole to defect states over 0.3 eV above the valence band would make it energetically unfavorable for transferring to PTZ.

It is interesting to compare the effect of electron and hole acceptors on the dynamics of single QDs. While both pathways shorten the exciton lifetime and reduce the average on-state lifetime of the QDs, they have different effects on the blinking dynamics of QDs. In QD−electron acceptor complexes, the electron transfer process leaves a hole in the QD, which increases the probability of gray and off-states.[29] However, unlike the hole acceptor, the electron acceptor cannot remove the hole in the dark state. Therefore, the net effect of electron acceptor is to increase the off-state probability densities in the QD−acceptor complexes, leading to a correlated electron transfer and QD blinking dynamics.

In summary, photoinduced hole transfer dynamics from single QDs to adsorbed phenothiazine molecules have been studied by single QD fluorescence spectroscopy. The hole transfer process was independently verified by ensemble-averaged transient absorption and fluorescence decay measurements. Single QD−PTZ complexes show fluctuation of fluorescence intensity and lifetime similar to those in free QDs. The hole transfer process shortens the lifetimes of on-states in the QD−hole acceptor complexes. There is a broad distribution of average hole transfer rates in different complexes, likely reflecting the distribution in the PTZ-to-QD ratio in the samples. Both the distributions of average hole transfer rates in single QD−PTZ complexes and ensemble-averaged fluorescence decay kinetics can be fit by a kinetics model that assumes a Poisson distribution of adsorbed PTZ molecules per QD, from which an average HT time of 50 ns in the 1:1 PTZ−QD complex was obtained. Unlike the correlated electron transfer and blinking dynamics observed in QD−electron acceptor complexes, the hole acceptors do not significantly alter the on- and off-state probability density distributions in the QD−PTZ complexes. Instead, it increases the probability of weakly emissive gray states. We attribute this to two competing effects of the hole acceptors. On one hand, the HT process generates a negatively charged QD, increasing the probability of gray and off-states. On the other hand, the hole acceptor can remove the hole in the off-state, reducing the probability of observing this state.

METHODS

Ensemble-Averaged Fluorescence Measurements and Nanosecond Transient Absorption. Ensemble-averaged fluorescence lifetimes of QDs and QD−PTZ complexes were measured in heptane solution in a 1 mm cuvette. The emission was detected by a microchannel plate photomultiplier tube (Hamamatsu R3809U-51), whose output was amplified and analyzed by a TCSPC board (Becker&Hickel SPC 600). Nanosecond transient absorption was performed with the EOS spectrometer (Ultrafast Systems LLC). The pump pulses at 400 nm were generated from the frequency-doubled output (~150 fs pulses at 800 nm) of a 1kHz Ti:sapphire laser system (Coherent Legend-H). The probe pulse (a 0.5 ns white light source operating at 1 kHz) was synchronized with the femtosecond amplifier, and the delay time was controlled by a digital delay generator. The probe light was detected using a fiber optics coupled multichannel spectrometer with CMOS sensor. The absorbance change was calculated from the intensities of sequential probe pulses with and without the 400 nm excitation.

Single QD Study. Single QD−PTZ complexes were studied with a home-built scanning confocal fluorescence microscope. Femtosecond laser pulses (~100 fs, 80 MHz repetition rate) were generated with a mode-locked Ti:sapphire laser (Tsunami oscillator pumped by 10 W Millennia Pro, Spectra-Physics). The repetition rate of output pulse centered at 1000 nm was reduced to 8.8 MHz using a pulse picker (Conoptics, USA). Excitation pulses at 500 nm were generated by second harmonic generation of the 1000 nm pulses in a BBO crystal. The excitation beam (~200 nW) was focused through an objective (100×, NA 1.4, oil immersion, Olympus) down to a

diffraction-limited spot on the sample, which was spin-coated onto the glass coverslips and placed on a piezo scanner (Mad City Laboratories). The resulting epifluorescence from the sample was detected by an avalanche photodiode (APD, Perkin-Elmer SPCM-AQR-14). The APD output was analyzed by a time-correlated single photon counting (TCSPC) board (Becker&Hickel SPC 600). The instrument response function for the fluorescence lifetime measurement had a full width at half-maximum of ~500 ps.

Sample Preparation. CdSe/CdS_{3ML}/$CdZnS_{2ML}$/ZnS_{2ML} core/multishell QD powders with first exciton absorption peak at 605 nm (capped by octadecylamine ligand) were obtained from Ocean NanoTech, LLC, USA. Phenothiazine was purchased from Sigma-Aldrich, USA. Three QD−PTZ samples, A, B, and C, were prepared for ensemble-averaged experiment, and the PTZ-to-QD ratios were controlled by adding different amount of PTZ to QD solutions (in heptanes). The mixtures were kept in the dark for 30 min before experiments. The samples (1, 2, and 3) for single QD studies were prepared in the same manner, with a much lower concentration of QDs (~10 pM). The solutions were spin-coated on glass coverslips for single QD studies.

Acknowledgment. The work was supported by the National Science Foundation (CHE-0848556) and Petroleum Research Fund (PRF#49286-ND6).

Supporting Information Available: Ensemble-averaged transient absorption spectra. This material is available free of charge *via* the Internet at http://pubs.acs.org.

REFERENCES AND NOTES

1. Pattantyus-Abraham, A. G.; Kramer, I. J.; Barkhouse, A. R.; Wang, X.; Konstantatos, G.; Debnath, R.; Levina, L.; Raabe, I.; Nazeeruddin, M. K.; Gratzel, M.; *et al.* Depleted-Heterojunction Colloidal Quantum Dot Solar Cells. *ACS Nano* **2010**, *4*, 3374–3380.
2. Sambur, J. B.; Novet, T.; Parkinson, B. A. Multiple Exciton Collection in a Sensitized Photovoltaic System. *Science* **2010**, *330*, 63–66.
3. Huynh, W. U.; Dittmer, J. J.; Alivisatos, A. P. Hybrid Nanorod−Polymer Solar Cells. *Science* **2002**, *295*, 2425–2427.
4. Robel, I.; Subramanian, V.; Kuno, M.; Kamat, P. V. Quantum Dot Solar Cells. Harvesting Light Energy with CdSe Nanocrystals Molecularly Linked to Mesoscopic TiO_2 Films. *J. Am. Chem. Soc.* **2006**, *128*, 2385–2393.
5. Kamat, P. Quantum Dot Solar Cells. Semiconductor Nanocrystals as Light Harvesters. *J. Phys. Chem. C* **2008**, *112*, 18737–18753.
6. Kamat, P. V.; Tvrdy, K.; Baker, D. R.; Radich, J. G. Beyond Photovoltaics: Semiconductor Nanoarchitectures for Liquid-Junction Solar Cells. *Chem. Rev.* **2010**, *110*, 6664–6688.
7. Tisdale, W. A.; Williams, K. J.; Timp, B. A.; Norris, D. J.; Aydil, E. S.; Zhu, X.-Y. Hot-Electron Transfer from Semiconductor Nanocrystals. *Science* **2010**, *328*, 1543–1547.
8. Boulesbaa, A.; Issac, A.; Stockwell, D.; Huang, Z.; Huang, J.; Guo, J.; Lian, T. Ultrafast Charge Separation at CdS Quantum Dot/Rhodamine B Molecule Interface. *J. Am. Chem, Soc.* **2007**, *129*, 15132–15133.
9. Huang, J.; Stockwell, D.; Huang, Z.; Mohler, D. L.; Lian, T. Photoinduced Ultrafast Electron Transfer from CdSe Quantum Dots to Re-Bipyridyl Complexes. *J. Am. Chem. Soc.* **2008**, *130*, 5632–5633.
10. Rossetti, R.; Beck, S. M.; Brus, L. E. Direct Observation of Charge-Transfer Reactions Across Semiconductor:Aqueous Solution Interfaces Using Transient Raman Spectroscopy. *J. Am. Chem. Soc.* **1984**, *106*, 980–984.
11. Rossetti, R.; Brus, L. E. Picosecond Resonance Raman Scattering Study of Methylviologen Reduction on the Surface of Photoexcited Colloidal CdS Crystallites. *J. Phys. Chem.* **1986**, *90*, 558–560.
12. Ramsden, J. J.; Gratzel, M. Formation and Decay of Methyl Viologen Radical Cation Dimers on the Surface of Colloidal CdS: Separation of Two- and Three-Dimensional Relaxation. *Chem. Phys. Lett.* **1986**, *132*, 269–272.
13. Henglein, A. Catalysis of Photochemical Reactions by Colloidal Semiconductors. *Pure Appl. Chem.* **1984**, *56*, 1215–1224.
14. Logunov, S.; Green, T.; Marguet, S.; El-Sayed, M. A. Interfacial Carriers Dynamics of CdS Nanoparticles. *J. Phys. Chem. A* **1998**, *102*, 5652–5658.
15. Burda, C.; Green, T. C.; Link, S.; El-Sayed, M. A. Electron Shuttling Across the Interface of CdSe Nanoparticles Monitored by Femtosecond Laser Spectroscopy. *J. Phys. Chem. B* **1999**, *103*, 1783–1788.
16. Kamat, P. V.; Dimitrijevic, N. M.; Fessenden, R. W. Photoelectrochemistry in Particulate Systems. 6. Electron-Transfer Reactions of Small CdS Colloids in Acetonitrile. *J. Phys. Chem.* **1987**, *91*, 396.
17. Blackburn, J. L.; Selmarten, D. C.; Nozik, A. J. Electron Transfer Dynamics in Quantum Dot/Titanium Dioxide Composites Formed by *In Situ* Chemical Bath Deposition. *J. Phys. Chem. B* **2003**, *107*, 14154–14157.
18. Robel, I.; Kuno, M.; Kamat, P. V. Size-Dependent Electron Injection from Excited CdSe Quantum Dots into TiO_2 Nanoparticles. *J. Am. Chem. Soc.* **2007**, *129*, 4136–4137.
19. Spanhel, l.; Weller, H.; Henglein, A. Photochemistry of Semiconductor Colloids. 22. Electron Injection from Illuminated CdS into Attached TiO_2 and ZnO Particles. *J. Am. Chem. Soc.* **1987**, *109*, 6632–6635.
20. Huang, J.; Huang, Z.; Jin, S.; Lian, T. Exciton Dissociation in CdSe Quantum Dots by Hole Transfer to Phenothiazine. *J. Phys. Chem. C* **2008**, *112*, 19734–19738.
21. Sharma, S. N.; Pillai, Z. S.; Kamat, P. V. Photoinduced Charge Transfer between CdSe Quantum Dots and *p*-Phenylenediamine. *J. Phys. Chem. B* **2003**, *107*, 10088–10093.
22. Landes, C. F.; Burda, C.; Braun, M.; El-Sayed, M. A. Photoluminescecne of CdSe Nanoparticles in the Presence of a Hole Acceptor: *n*-Butylamine. *J. Phys. Chem. B* **2001**, *105*, 2981.
23. Landes, C. F.; Braun, M.; El-Sayed, M. A. On the Nanoparticle to Molecular Size Transition: Fluorescence Quenching Studies. *J. Phys. Chem. B* **2001**, *105*, 10554–10558.
24. Guyot-Sionnest, P. Intraband Spectroscopy and Semiconductor Nanocrystals. *Struct. Bonding* **2005**, *118*, 59–77.
25. Issac, A.; Jin, S.; Lian, T. Intermittent Electron Transfer Activity from Single CdSe/ZnS QDs. *J. Am. Chem. Soc.* **2008**, *130*, 11280–11281.
26. Cui, S.-C.; Tachikawa, T.; Fujitsuka, M.; Majima, T. Interfacial Electron Transfer Dynamics in a Single CdTe Quantum Dot-Pyromellitimide Conjugate. *J. Phys. Chem. C* **2008**, *112*, 19625–19634.
27. Jin, S.; Lian, T. Electron Transfer Dynamics from Single CdSe/ZnS Quantum Dots to TiO_2 Nanoparticles. *Nano Lett.* **2009**, *9*, 2448–2454.
28. Jin, S.; Song, N.; Lian, T. Suppressed Blinking Dynamics of Single QDs on ITO. *ACS Nano* **2010**, *4*, 1545–1552.
29. Jin, S.; Hsiang, J.-C.; Zhu, H.; Song, N.; Dickson, R. M.; Lian, T. Correlated Single Quantum Dot Blinking and Interfacial Electron Transfer Dynamics. *Chem. Sci.* **2010**, *1*, 519–526.
30. Cui, S.-C.; Tachikawa, T.; Fujitsuka, M.; Majima, T. Photoinduced Electron Transfer in a Quantum Dot−Cucurbituril Supramolecular Complex. *J. Phys. Chem. C* **2011**, *115*, 1824–1830.
31. Song, N.; Zhu, H.; Jin, S.; Zhan, W.; Lian, T. Poisson-Distributed Electron-Transfer Dynamics from Single Quantum Dots to C60 Molecules. *ACS Nano* **2011**, *5*, 613–21.
32. Nirmal, M.; Dabbousi, B. O.; Bawendi, M. G.; Macklin, J. J.; Trautman, J. K.; Harris, T. D.; Brus, L. E. Fluorescence Intermittency in Single Cadmium Selenide Nanocrystals. *Nature* **1996**, *383*, 802–804.
33. Shimizu, K. T.; Neuhauser, R. G.; Leatherdale, C. A.; Empedocles, S. A.; Woo, W. K.; Bawendi, M. G. Blinking Statistics in Single Semiconductor Nanocrystal Quantum Dots. *Phys. Rev. B* **2001**, *63*, 205316/1–205316/5.
34. Krauss, T. D.; O'Brien, S.; Brus, L. E. Charge and Photoionization Properties of Single Semiconductor Nanocrystals. *J. Phys. Chem. B* **2001**, *105*, 1725–1733.
35. Empedocles, S.; Bawendi, M. Spectroscopy of Single CdSe Nanocrystallites. *Acc. Chem. Res.* **1999**, *32*, 389–396.

36. Shimizu, K. T.; Woo, W. K.; Fisher, B. R.; Eisler, H. J.; Bawendi, M. G. Surface-Enhanced Emission from Single Semiconductor Nanocrystals. *Phys. Rev. Lett.* **2002**, *89*, 117401/1–117401/4.
37. Chen, Y.; Vela, J.; Htoon, H.; Casson, J. L.; Werder, D. J.; Bussian, D. A.; Klimov, V. I.; Hollingsworth, J. A. "Giant" Multishell CdSe Nanocrystal Quantum Dots with Suppressed Blinking. *J. Am. Chem. Soc.* **2008**, *130*, 5026–5027.
38. Mahler, B.; Spinicelli, P.; Buil, S.; Quelin, X.; Hermier, J.-P.; Dubertret, B. Towards Non-blinking Colloidal Quantum Dots. *Nat. Mater.* **2008**, *7*, 659.
39. Hohng, S.; Ha, T. Near-Complete Suppression of Quantum Dot Blinking in Ambient Conditions. *J. Am. Chem. Soc.* **2004**, *126*, 1324–1325.
40. Wang, X.; Ren, X.; Kahen, K.; Hahn, M. A.; Rajeswaran, M.; Maccagnano-Zacher, S.; Silcox, J.; Cragg, G. E.; Efros, A. L.; Krauss, T. D. Non-blinking Semiconductor Nanocrystals. *Nature* **2009**, *459*, 686.
41. Odoi, M. Y.; Hammer, N. I.; Early, K. T.; McCarthy, K. D.; Tangirala, R.; Emrick, T.; Barnes, M. D. Fluorescence Lifetimes and Correlated Photon Statistics from Single CdSe/Oligo(phenylene vinylene) Composite Nanostructures. *Nano Lett.* **2007**, *7*, 2769–2773.
42. Hammer, N. I.; Early, K. T.; Sill, K.; Odoi, M. Y.; Emrick, T.; Barnes, M. D. Coverage-Mediated Suppression of Blinking in Solid State Quantum Dot Conjugated Organic Composite Nanostructures. *J. Phys. Chem. B* **2006**, *110*, 14167–14171.
43. Ray, K.; Badugu, R.; Lakowicz, J. R. Metal-Enhanced Fluorescence from CdTe Nanocrystals: A Single-Molecule Fluorescence Study. *J. Am. Chem. Soc.* **2006**, *128*, 8998–8999.
44. Fomenko, V.; Nesbitt, D. J. Solution Control of Radiative and Nonradiative Lifetimes: A Novel Contribution to Quantum Dot Blinking Suppression. *Nano Lett.* **2008**, *8*, 287–293.
45. Efros, A. L.; Rosen, M. Random Telegraph Signal in the Photoluminescence Intensity of a Single Quantum Dot. *Phys. Rev. Lett.* **1997**, *78*, 1110–1113.
46. Fisher, B. R.; Eisler, H.-J.; Stott, N. E.; Bawendi, M. G. Emission Intensity Dependence and Single-Exponential Behavior in Single Colloidal Quantum Dot Fluorescence Lifetimes. *J. Phys. Chem. B* **2004**, *108*, 143–148.
47. Issac, A.; von Borczyskowski, C.; Cichos, F. Correlation between Photoluminescence Intermittency of CdSe Quantum Dots and Self-Trapped States in Dielectric Media. *Phys. Rev. B* **2005**, *71*, 161302/1–161302/4.
48. Kuno, M.; Fromm, D. P.; Johnson, S. T.; Gallagher, A.; Nesbitt, D. J. Modeling Distributed Kinetics in Isolated Semiconductor Quantum Dots. *Phys. Rev. B* **2003**, *67*, 125304/1–125304/15.
49. Montiel, D.; Yang, H. Observation of Correlated Emission Intensity and Polarization Fluctuations in Single CdSe/ZnS Quantum Dots. *J. Phys. Chem. A* **2008**, *112*, 9352–9355.
50. Peterson, J. J.; Nesbitt, D. J. Modified Power Law Behavior in Quantum Dot Blinking: A Novel Role for Bi-excitons and Auger Ionizatoin. *Nano Lett.* **2009**, *9*, 338–345.
51. Schlegel, G.; Bohnenberger, J.; Potapova, I.; Mews, A. Fluorescence Decay Time of Single Semiconductor Nanocrystals. *Phys. Rev. Lett.* **2002**, *88*, 137401-1.
52. Tang, J.; Marcus, R. A. Determination of Energetics and Kinetics from Single-Particle Intermittency and Ensemble-Averaged Fluorescence Intensity Decay of Quantum Dots. *J. Chem. Phys.* **2006**, *125*, 044703/1–044703/8.
53. Verberk, R.; van Oijen, A. M.; Orrit, M. Simple Model for the Power-Law Blinking of Single Semiconductor Nanocrystals. *Phys. Rev. B* **2002**, *66*, 233202/1–233202/4.
54. Zhang, K.; Chang, H.; Fu, A.; Alivisatos, A. P.; Yang, H. Continuous Distribution of Emission States from Single CdSe/ZnS Quantum Dots. *Nano Lett.* **2006**, *6*, 843–847.
55. Kuno, M.; Fromm, D. P.; Hamann, H. F.; Gallagher, A.; Nesbitt, D. J. "On"/"Off" Fluorescence Intermittency of Single Semiconductor Quantum Dots. *J. Chem. Phys.* **2001**, *115*, 1028–1040.
56. Tang, J.; Marcus, R. A. Single Particle Versus Ensemble Average: From Power-Law Intermittency of a Single Quantum Dot to Quasistretched Exponential Fluorescence Decay of an Ensemble. *J. Chem. Phys.* **2005**, *123*, 204511/1–204511/6.
57. Tang, J.; Marcus, R. A. Diffusion-Controlled Electron Transfer Processes and Power-Law Statistics of Fluorescence Intermittency of Nanoparticles. *Phys. Rev. Lett.* **2005**, *95*, 107401/1–107401/4.
58. Tang, J.; Marcus, R. A. Mechanisms of Fluorescence Blinking in Semiconductor Nanocrystal Quantum Dots. *J. Chem. Phys.* **2005**, *123*, 054704/1–054704/12.
59. Garcia-Santamaria, F.; Chen, Y.; Vela, J.; Schaller, R. D.; Hollingsworth, J. A.; Klimov, V. I. Suppressed Auger Recombination in "Giant" Nanocrystals Boosts Optical Gain Performance. *Nano Lett.* **2009**, *9*, 3482–3488.
60. Ito, Y.; Matsuda, K.; Kanemitsu, Y. Mechanism of Photoluminescence Enhancement in Single Semiconductor Nanocrystals on Metal Surfaces. *Phys. Rev. B* **2007**, *75*, 033309.
61. Bharadwaj, P.; Novotny, L. Robustness of Quantum Dot Power-Law Blinking. *Nano Lett.* **2011**, *11*, 2137–2141.
62. Brus, L. A Simple Model for the Ionization Potential, Electron Affinity, and Aqueous Redox Potentials of Small Semiconductor Crystallites. *J. Chem. Phys.* **1983**, *79*, 5566–5571.
63. Brus, L. E. Electron–Electron and Electron–Hole Interactions in Small Semiconductor Crystallites: The Size Dependence of the Lowest Excited Electronic State. *J. Chem. Phys.* **1984**, *80*, 4403–4409.
64. Tierney, M. T.; Grinstaff, M. W. Synthesis and Characterization of Fluorenone-, Anthraquinone-, and Phenothiazine-Labeled Oligodeoxynucleotides: 5′-Probes for DNA Redox Chemistry. *J. Org. Chem.* **2000**, *65*, 5355–5359.
65. Klimov, V. I. Spectral and Dynamical Properties of Multiexcitons in Semiconductor Nanocrystals. *Annu. Rev. Phys. Chem.* **2007**, *58*, 635–673.
66. Klimov, V. I.; Mikhailovsky, A. A.; McBranch, D. W.; Leatherdale, C. A.; Bawendi, M. G. Quantization of Multiparticle Auger Rates in Semiconductor Quantum Dots. *Science* **2000**, *287*, 1011–1013.
67. Drndic, M.; Wang, S.; Querner, C.; Fischbein, M. D.; Willis, L.; Novikov, D. S.; Crouch, C. H. Blinking Statistics Correlated with Nanoparticle Number. *Nano Lett.* **2008**, *8*, 4020–4026.
68. Drndic, M.; Wang, S.; Querner, C.; Dadosh, T.; Crouch, C. H.; Novikov, D. S. Collective Fluorescence Enhancement in Nanoparticle Clusters. *Nat. Comm.* **2011**, *2*, 364.
69. Boulesbaa, A.; Huang, Z.; Wu, D.; Lian, T. Competition between Energy and Electron Transfer from CdSe QDs to Adsorbed Rhodamine B. *J. Phys. Chem. A* **2010**, *114*, 962–969.
70. Pons, T.; Medintz, I. L.; Wang, X.; English, D. S.; Mattoussi, H. Solution-Phase Single Quantum Dot Fluorescence Resonance Energy Transfer. *J. Am. Chem. Soc.* **2006**, *128*, 15324–15331.
71. Zhu, H.; Song, N.; Lian, T. Controlling Charge Separation and Recombination Rates in CdSe/ZnS Type I Core–Shell Quantum Dots by Shell Thicknesses. *J. Am. Chem. Soc.* **2010**, *132*, 15038–15045.
72. Tang, J.; Lee, D. H.; Yuan, C. T.; Tachiya, M. Influence of Bin Time and Excitation Intensity on Fluorescence Lifetime Distribution and Blinking Statistics of Single Quantum Dots. *Appl. Phys. Lett.* **2009**, 95.
73. Frantsuzov, P. A.; Volkan-Kacso, S.; Janko, B. Model of Fluorescence Intermittency of Single Colloidal Semiconductor Quantum Dots Using Multiple Recombination Centers. *Phys. Rev. Lett.* **2009**, 103.
74. Tang, J.; Lee, D. H.; Yeh, Y. C.; Yuan, C. T. Short-Time Power-Law Blinking Statistics of Single Quantum Dots and a Test of the Diffusion-Controlled Electron Transfer Model. *J. Chem. Phys.* **2009**, 131.
75. Crouch, C. H.; Sauter, O.; Wu, X. H.; Purcell, R.; Querner, C.; Drndic, M.; Pelton, M. Facts and Artifacts in the Blinking Statistics of Semiconductor Nanocrystals. *Nano Lett.* **2010**, *10*, 1692–1698.
76. Ma, X.; Tan, H.; Kipp, T.; Mews, A. Fluorescence Enhancement, Blinking Suppression, and Gray States of Individual Semiconductor Nanocrystals Close to Gold Nanoparticles. *Nano Lett.* **2010**, *10*, 4166–4174.

77. Gómez, D. E.; van Embden, J.; Mulvaney, P.; Fernée, M. J.; Rubinsztein-Dunlop, H. Exciton-Trion Transitions in Single CdSe−CdS Core−Shell Nanocrystals. *ACS Nano* **2009**, *3*, 2281–2287.
78. Jha, P. P.; Guyot-Sionnest, P. Trion Decay in Colloidal Quantum Dots. *ACS Nano* **2009**, *3*, 1011–1015.
79. Marcus, R. A.; Sutin, N. Electron Transfers in Chemistry and Biology. *Biochem. Biophys. Acta* **1985**, *811*, 265–322.